International Journal of Academic Health and Medical Research (IJAHMR)
ISSN: 2643-9824
Vol. 8 Issue 2 February - 2024, Pages: 1-11

A Review of Integrated Transceiver Circuits for Medical Ultrasound Application in Low-Income Countries

Kibirige David[1],Opolot Samuel Otekat[2], Kanyana Ruth[3], , Kolokolo Hannington[4], Shema Innocent[5], Kalule Mugagga[6], Tigasitwa Fred[7], Wodidi Jonah[8] ,Senyonjo Timothy[8],Kwesiga Dominic[10]

Ernest Cook Ultrasound Research and Education Institute (ECUREI)
Department of Engineering and biomedical sciences
semkibirige@gmail.com[1] ,Samueloso63@gmail.com[2], kanyanaruth@gmail.com[3], , hanningtonkolokolo@gmail.com[4], shemablast10@gmail.com[5],Vicamugagga@gmail.com[6] , ftigasitwa@gmail.com[7] ,wodidijona@gmail.com [8], timothysenyonjo387@gmail.com[9] ,kabsdominique@gmail.com[10],
U/23030031/MBE[1] ,U/23030034/MBE[2], U/23030023/MBE[3], , U/23030029/MBE[4,] U/23030022/MBE[5], U/23030045/MBE[6], U/23030049/MBE[7], U/23030041/MBE[8], U/23030044/MBE[9], U/23030047/MBE[10]

Abstract*: The shift in medical ultrasound imaging from traditional cart-based scanners to newer formats like imaging catheters, hand-held point-of-care scanners, and ultrasound patches has created a growing demand for integrated transceivers. These transceivers must be closely integrated with the transducer to achieve channel-count reduction, improve signal quality, and potentially enable full digitization. This research paper examines compact and power-efficient circuit solutions for these integrated transceivers. The paper commences with a concise overview of ultrasound transducer technologies and the fundamental principles governing the ultrasound transmit-receive signal path. Regarding transmission, it explores various high-voltage pulsers, ranging from compact unipolar pulsers to multi-level pulsers that offer amplitude control and enhanced power efficiency. On the receive circuits side, the discussion begins with low-noise amplifiers, which serve as the power- and performance-limiting building block. The paper also addresses solutions for time-gain compensation, which play a vital role in reducing signal dynamic range by compensating for the decreasing echo-signal amplitude associated with propagation attenuation. Moreover, the paper explores the option of directly digitizing the echo signal at the transducer. Finally, it concludes by reflecting on the future opportunities and challenges in the realm of integrated circuits for ultrasound applications.*

Keywords*: Transducer, ultrasound, amplifier, integrated circuits, power efficiency*

1. INTRODUCTION

Ultrasound imaging plays a crucial role in medical applications, aiding in diagnosis and guiding treatments in fields like obstetrics and cardiology. Despite its long history, significant developments are on the horizon that will revolutionize ultrasound usage. One notable change is in the form factor, shifting from traditional hand-held probes connected to bulky imaging systems to more compact and portable options, including pocket-sized handheld scanners, endoscopes, catheters, pills, and patches (Fig. 1). Another significant advancement is the transition from 2D to 3D imaging [5]. While 2D cross-sectional images were conventionally produced using 1D transducer arrays, the increasing prevalence of 2D arrays allows for the generation of 3D images, not only in hand-held probes but also in miniature probes like endoscopes and imaging catheters. Additionally, there is a trend toward making ultrasound more accessible beyond expert sonographers, aiming for broader clinical use and eventually use by the general public, which necessitates cost reduction and enhanced user-friendliness [3].

Integrated circuits play a pivotal role in driving these advancements [21]. The electronics architecture of conventional imaging systems, relying on commercial off-the-shelf components, lacks scalability for the new form factors concerning size and power consumption. Moreover, their channel count is not adaptable to 3D imaging requirements. Integrated transceiver circuits, closely integrated with the ultrasound transducer array, offer a solution to these challenges [21]. These circuits pave the way for scaling down the technology, especially when combined with the shift from labor-intensive and costly bulk-piezoelectric transducers to micro-machined transducers, thereby enabling more widespread and cost-effective use [2]. This paper presents a review of recent developments in integrated ultrasound transceiver design. Section II begins with an examination of transducer technologies and ultrasound system architectures, emphasizing the crucial role of integrated transceivers in enabling new applications and aligning system requirements with front-end building-block specifications.

International Journal of Academic Health and Medical Research (IJAHMR)
ISSN: 2643-9824
Vol. 8 Issue 2 February - 2024, Pages: 1-11

Figure 1: Examples of emerging medical ultrasound imaging devices (clockwise from the left): a hand-held point-of-care ultrasound scanner (image courtesy of Butterfly Network) [11]; a 3D intra-cardiac imaging catheter [9]; an artist's impression of a 3D transesophageal ultrasound probe [14]; a pill-shaped ultrasonic endoscopy device (image courtesy of Univ. of Glasgow) [2]; an artist's impression of a wearable ultrasound patch (image courtesy of ULIMPIA project)

2. **ULTRASOUND SYSTEM ARCHITECTURE**

A. ULTRASOUND TRANSDUCERS

In an ultrasound imaging system, the transducer has a dual role: emitting acoustic waves into the body and capturing the returning echo signals [18]. The arrival time of an echo provides information about its depth of origin, but lateral resolution of objects or scatterers is achieved through beamforming. To accomplish this, ultrasound transducers are typically divided into an array of elements.

For 2D imaging, 1D array (linear arrays or phased arrays) with up to 256 elements are used. However, to achieve 3D imaging without relying on mechanical translation or rotation of a 1D array, a 2D array (also known as a matrix transducer) is necessary, and this type can consist of thousands of elements [18]. The overall size (aperture) of the array is crucial for determining the field of view and spatial resolution needed. On the other hand, the element pitch is determined by beamforming requirements, particularly to avoid grating lobes. For phased-array transducers, this means that a pitch of about half the wavelength is necessary.

The majority of ultrasound probes in use nowadays are based on bulk piezoelectric transducers (Fig. 2a) . A layer of piezoelectric material, typically a piezoceramic such as lead-zirconate-titanate (PZT) or a piezocomposite, is mechanically diced into elements and equipped with top and bottom electrodes. An AC voltage applied to these electrodes is converted into a pressure wave through the piezoelectric effect, while, conversely, an incoming pressure wave can be detected as a charge displacement or voltage change on the electrodes [10]. Mechanically, such a transducer is a thickness-mode resonator tuned to the frequency range of interest, typically with a low-quality factor to allow trans-mission of short pulses. To ensure effective coupling of the acoustic waves into the medium in spite of mismatches in acoustic impedance, backing and matching layers are used [10]. Fabrication of bulk piezoelectric transducer arrays, in particular 2D arrays, is relatively complex, time-consuming, and hence expensive.

To overcome these fabrication challenges, wafer-scale batch-fabrication techniques have been explored extensively as an alternative [2]. The resulting micro-machined ultrasound transducers (MUTs) are based on a thin flexible membrane fabricated using surface or bulk micro-machining techniques [2]. In the case of piezoelectric MUTs (PMUTs), a thin piezoelectric film with electrodes is deposited on the membrane (Fig. 2b) [16].

In the case of capacitive MUTs (CMUTs), the membrane is electrostatically actuated by means of electrodes in the membrane and in the substrate underneath (Fig. 2c) [13]. Typically, a relatively large DC bias voltage is applied to statically deflect the membrane and linearize its behavior. A smaller superimposed AC voltage is used for transmission, while for reception, the charge displacement due to capacitance changes associated with membrane deflection is detected.

In spite of their very different operating principles, the electrical impedance of all three mentioned transducer types can be modeled, to first order, using a so-called Butterworth Van-Dyke model (Fig. 2d), which includes a resonant branch (Rm, Lm, Cm) that models the mechanical resonance of the transducer, and a capacitor (Cp) that represents its electrical capacitance [2]. This single-port model proves useful in modeling the load that the transducer represents at the output of a transmit circuit, and in modeling of the transducer as a small-signal source at the input of an LNA, where a source can be included in the resonant branch to represent the acoustic input, and the thermal noise associated with Rm represents the noise contribution of the transducer. For a more accurate representation of the acoustic domain, a two-port model can be adopted.

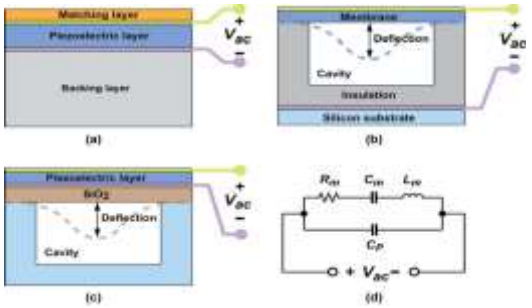

Figure 2: Schematic representation of (a) a bulk piezoelectric transducer, (b) a capacitive micromachine ultrasound transducer (CMUT), (c) a piezoelectric micromachined ultrasound transducer (PMUT), and (d) the Butterworth-Van Dyke equivalent circuit model.

B. CONVENTIONAL ULTRASOUND IMAGING SYSTEMS

Fig. 3 depicts a schematic diagram of a conventional ultrasound imaging system linked to a probe comprising an array of N transducer elements, each responsible for transmitting (TX) and receiving (RX) acoustic waves. These elements are interconnected using cables to transceiver channels within the imaging system. During transmission, the elements are activated by pulses, which are timed using a TX beamformer to achieve the desired spatial distribution of the acoustic wave. Typically, the wave is focused at a specific point along the scan line to be imaged [7].

To ensure that detectable echo signals are obtained even at the deepest point of the image, where propagation attenuation significantly reduces signal amplitude, the transducer elements are driven with high-voltage (HV) pulses [7]. These pulses have amplitudes ranging from tens of volts to over 100 V. During pulse transmission, transmit/receive (T/R) switches are employed to protect the receive circuits.

Subsequently transmitting ultrasound waves, the returning echo signals received by each transducer element undergo amplification using a low-noise amplifier (LNA) [7]. In an attenuating medium like the human body, the first echoes to reach the probe come from nearby scatterers, resulting in higher amplitudes compared to echoes arriving later from deeper scatterers that undergo more propagation attenuation. To compensate for this decreasing amplitude, a time-gain compensation (TGC) amplifier is utilized, which applies a linear-in-dB gain that increases with time [7]. This effectively reduces the dynamic range of the signals. The echo signals are then converted into digital form by an analog-to-digital converter (ADC), typically preceded by an anti-aliasing filter (not shown in Fig. 3).

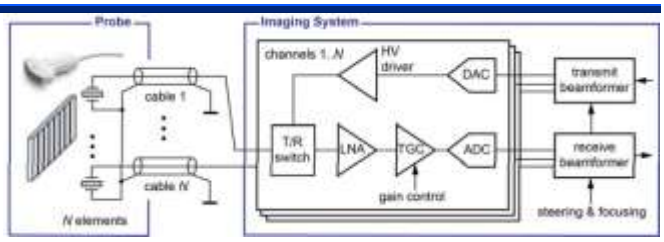

Figure 3: Block diagram of a conventional ultrasound imaging system

Subsequently, an RX beamformer combines the digitized echo signals, typically through a delay-and-sum operation, to constructively add signals from the desired focal point while suppressing signals from other locations. The output of the RX beamformer is further processed to create an image [1]. In the case of brightness-mode (B-mode) imaging, both the TX and RX beamformers focus on a point along a scan line in the medium [2]. The envelope detection of the RX beamformer's output yields the image brightness along the corresponding line in the image. Multiple scan lines are combined to form the complete image, and each requires a cycle of pulse transmission and echo reception [1].

The architectural setup shown in Fig. 3 restricts the number of elements in the system due to the one-to-one correspondence between transducer elements, cables, and transceiver channels. Practical limitations in cable count and system size allow for a maximum of 256 elements in high-end imaging systems. This limitation hinders the use of matrix transducers, necessary for 3D imaging, which typically consist of thousands of elements.

The integration of Application-Specific Integrated Circuits (ASICs) into ultrasound probes serves as a crucial means to bridge the gap between the high number of transducer elements required for 3D imaging and the limited number of system channels (Fig. 4a) [17]. To achieve this, various approaches have been employed, such as multiplexing and sub-array beamforming. In such cases, the ASIC generates analog output signals for the imaging system. Furthermore,

ASICs contribute to enhancing the signal-to-noise ratio (SNR) by locally amplifying the echo signals received by the transducer elements [17]. This approach prevents signal attenuation associated with connecting the small, high-impedance elements of a matrix transducer to long cables.

Beyond channel-count reduction, in-probe ASICs offer additional functionalities. For instance, they can facilitate full digitization (Fig. 4b) and perform further processing of the echo signals. This becomes particularly crucial for portable ultrasound probes, where the traditional imaging system with analog front-ends and ADCs has been replaced by smartphones or tablets. As a result, the data acquisition functionality, traditionally implemented in the imaging system, now transitions into the ASIC, while image processing takes place in software.

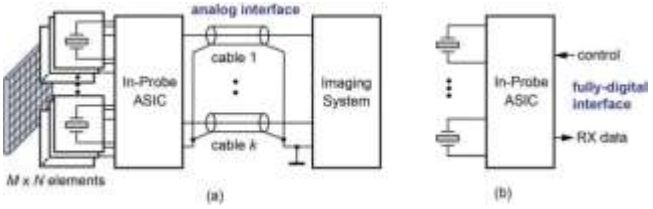

Figure 4: Smart ultrasound probe with in-probe ASIC

C. INTEGRATED CIRCUITS IN THE PROBE TRADE-OFFS IN TRANSCEIVER DESIGN

Key building blocks of any in-probe ASIC are the element-level transceiver circuits. They determine to a large extent the performance in terms of SNR, and tend to domi- nate power consumption, and should therefore be carefully optimized.

Essential for this optimization is the analysis of the transmit-receive signal path, a typical example of which is illustrated in Fig. 5, in which each transducer element is driven by a pulser. The pressure generated at the surface of the elements depends on the amplitude of the applied pulse, and the transmit efficiency (expressed in Pa/V) of the transducer. In the case of focused transmission, the pulses.

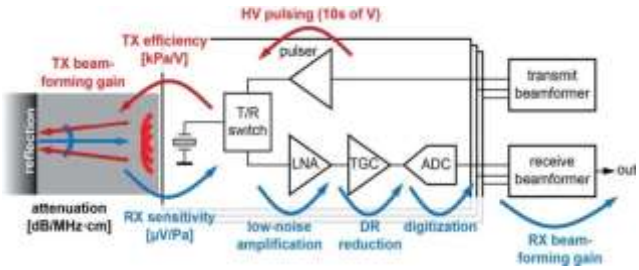

Figure 5: Transmit-receive signal path (with pulse transmission in red, and echo reception in blue).

The transmit beamformer carefully times the acoustic waves to converge at the desired focal point. Calculating the pressure at this point involves considering the transmit beamforming gain and the propagation attenuation within the medium.

As the acoustic wave encounters interfaces between regions with different acoustic impedance in the medium, it produces echoes that return to the transducer. The amplitude of each echo depends on the interface's reflection coefficient and the geometrical spreading and attenuation experienced during its journey back to the transducer. This surface pressure is then converted to a voltage through the transducer's receive sensitivity (measured in V/Pa). The resulting signal undergoes amplification by the LNA and TGC, followed by digitization. The signals from different elements are then combined by the receive beamformer. Correlated signals add up constructively, resulting in the RX beamforming gain, while uncorrelated noise is suppressed. Note that alternative configurations are possible, where part of the beamforming is done in the analog domain before digitization.

The system depicted in Fig. 5 involves numerous design parameters that must be carefully chosen to achieve the desired SNR at the output of the RX beamformer while minimizing power consumption. In a given array configuration, using a specific beamforming scheme and transducer characteristics, the amplitude of the signal received by an individual transducer element is mainly determined by the TX pulse's amplitude, while the noise floor is limited by

the element's noise. The final SNR is influenced by the noise figure (NF) of the receive circuits, which can be improved at the cost of higher power consumption, and enhanced by the RX beamforming gain.

Ideally, a minimum TX amplitude can achieve the desired SNR when receive circuits are noise-free (NF of 0 dB). However, in practical scenarios, the TX amplitude needs to be set higher to account for a realistic NF, leading to a trade-off between TX and RX power consumption. Although the practical TX amplitude may already reach tens of Volts, necessitating HV pulsers implemented in special HV CMOS technology, the average TX power consumption is typically not dominant due to the brief duration of pulse transmission compared to echo reception.

3. INTEGRATED TRANSMITTER CIRCUITS

In conventional ultrasound systems, the generation of high-voltage (HV) signals to drive the transducer elements occurs within the imaging system. However, the novel devices discussed in this paper necessitate the integration of transmit (TX) functionality closer to the transducer. This integration can be achieved through HV switching or multiplexing, where multiple transducer elements connect to a single TX channel in the imaging system [15]; [20]. Nevertheless, to avoid reducing the frame rate due to multiplexing, it is preferable to generate the HV signals at the element level.

Ultrasound transmitter circuits can be classified into two categories, namely pulsers and linear amplifiers, depending on the type of voltage waveform required. While both categories have found extensive use in discrete-circuit ultrasound systems, pulsers have been more commonly adopted in integrated systems due to their simplicity and superior power efficiency. Advancements in solid-state circuit technologies, particularly the rapid expansion of high-voltage process options, have enabled several new on-chip transmitter solutions that cater to the diverse demands of emerging integrated ultrasound systems. This section provides an overview of the latest developments in integrated transmitter circuits, with a special emphasis on emerging techniques for pulser design.

A. SQUARE-WAVE PULSERS

The square-wave pulser serves as the simplest transmitter architecture, generating a wide-band excitation voltage that alternates between two fixed or varying voltage levels. Initially adopted in integrated ultrasound transceivers for their simplicity, unipolar square-wave pulsers produce output swinging between ground potential and a single high-voltage (HV) supply, either positive or negative [19]. Various implementations have been explored to achieve compactness and efficiency in unipolar pulsers. However, some of these designs suffer from power waste during low output states and limited pulse rising time when interfacing with capacitive loads [22].

Bipolar pulsers have emerged as a solution to address the limitations of unipolar pulsers [21]. In contrast to unipolar pulsers, bipolar pulsers generate excitation signals that symmetrically transit between positive and negative HV voltage levels. This approach eliminates the DC component in the output waveforms, resulting in a more efficient distribution of transmitted energy and improved round-trip signal-to-noise ratio (SNR) [21]. Additionally, bipolar pulsers are compatible with various advanced imaging techniques, such as tissue harmonic imaging, pulse inversion, and chirp coding.

The typical implementation of a bipolar pulser involves using either an HV inverter or a source-follower-based push-pull stage with positive and negative HV supplies as the front-end stage. These designs offer enhanced performance and versatility, making them favorable choices for integrated ultrasound transceivers.

B. MULTI-LEVEL PULSERS

The significance of multi-level pulsing (Fig. 6) is increasing in integrated ultrasound imagers due to several advantages.

Firstly, it improves transmission linearity, resulting in better image quality.Secondly, it allows temporal and spatial apodization, leading to sidelobe reduction and enhanced contrast in the reconstructed image [12].Additionally, certain multi-level pulsing techniques can save dynamic power dissipation by recycling part of the charge during voltage transitions . This is particularly beneficial for CMUTs operating in the collapse mode as it improves device reliability.

A 3-level pulser, the simplest form of multi-level pulsers, can be achieved by adding return-to-zero (RZ) switching to a bipolar square-wave pulser. Several designs have been proposed to achieve this. One approach involves a direct discharging path from the transducer to ground via a high-voltage (HV) floating-gate driver and a grounding switch. Another design adds the grounding switch to the output of a pre-driver stage [12]. However, this eliminates potential power savings. Alternatively, the charge-recycling pulser concept utilizes (N-1) HV switches, each connected to a regulated voltage source, to charge and discharge the transducer in steps, reducing dynamic power consumption by a factor of N-1. Although this approach offers energy savings, it requires excessive HV switches for N > 3, leading to significant silicon area and driving power challenges.

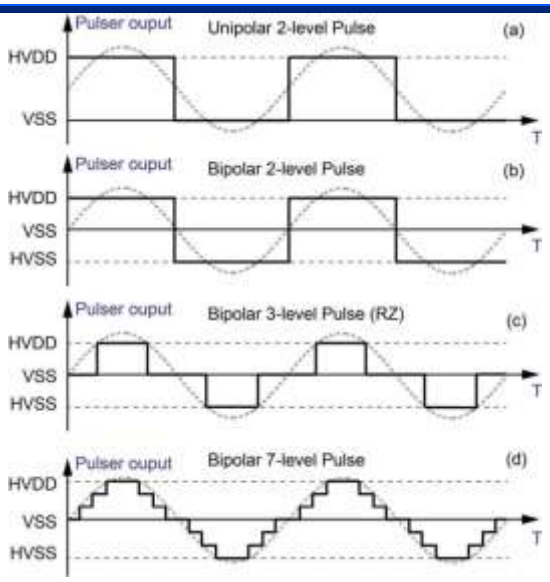

Figure 6: Typical pulse waveforms: (a) unipolar 2-level; (b) bipolar 2-level; (c) bipolar 3-level with return-to-zero; (d) bipolar 7-level

An alternative charge-recycling mechanism involves shorting the two electrodes of a differential PMUT element to discharge it, reducing energy expenditure on charging and discharging parasitic capacitance to ground [12]. Another proposed approach, the capacitive supply-multiplication scheme, substantially reduces power consumption but requires large capacitors. Additionally, energy stored on the transducer capacitance can be recycled using an inductor, providing significant power savings, but the need for an off-chip inductor limits its use in transducer arrays.

In an integrated ultrasound imaging system with a low transmit/receive (TX/RX) duty cycle, where transmission does not dominate power consumption, designers have room to trade dynamic energy savings for a more compact multi-level pulser. One such proposal is the feedback-based 7-level pulser, which utilizes a capacitive voltage divider to scale down the HV pulser output voltage. It operates with a zero-crossing-detector (ZCD) and a digital feedback controller, allowing accurate control of the transducer voltage. The absence of HV transistors and off-chip HV supplies makes

this approach highly suitable for compact multi-level pulsers, especially when closely integrated with CMUT arrays.

4. INTEGRATED RECEIVERS

A. LOW-NOISE AMPLIFIERS

In most integrated ultrasound systems, the first building block in the receive chain that interfaces directly with the transducer is the Low-Noise Amplifier (LNA) [19].Its primary function is to provide linear amplification of the echo signals to suppress noise from subsequent circuits. Depending on the transducer's impedance characteristics and the desired output format for further signal processing, this amplification can be implemented as a voltage gain, current gain, transimpedance gain, or transconductance gain. As the LNA significantly affects the noise performance of the integrated receiver, it demands a substantial amount of power and area to ensure a suitable Noise Figure (NF) for the entire system. Often, the majority of the receiver power is consumed by the LNA. To select an optimal LNA topology, a thorough understanding of the transducer characteristics is necessary to strike a balance between noise, power, and area considerations.

Among different LNA architectures, voltage amplifiers (VA) (Fig. 7a) and transconductance amplifiers (TCA) (Fig. 7b) sense the transducer's voltage by providing a relatively high input impedance . On the other hand, transimpedance amplifiers (TIA) (Fig. 7c) and current amplifiers (CA) (Fig. 7d) sense the current by establishing a low input impedance virtual ground. In integrated systems, VAs and TCAs are commonly used for transducers with lower impedance (less than 2 kΩ), such as PZTs and PMUTs [19]. Meanwhile, TIAs and CAs are preferred for transducers like CMUTs and polyvinylidene fluorides (PVDF) transducers, which typically exhibit higher impedance (above 10 kΩ) [15]. It is important to note that transducer impedance is a complex function dependent on physical dimensions, material, fabrication process, and acoustic load. Therefore, for custom integrated systems, a tailored analysis based on the specific transducer impedance profile is essential to determine the optimal topology. For instance, for fine-pitch PZTs used in high-frequency IVUS applications, a relatively high impedance (5 kΩ) makes current sensing with a TIA a more energy-efficient choice.

To enhance the noise-power trade-off and area-efficiency of the LNA, various circuit techniques have been developed. Capacitive feedback, for instance, has been utilized in both VAs and TIAs to eliminate common noise sources and improve performance [12]. These techniques play a critical role in achieving high-quality ultrasound imaging with efficient power consumption and reduced noise.

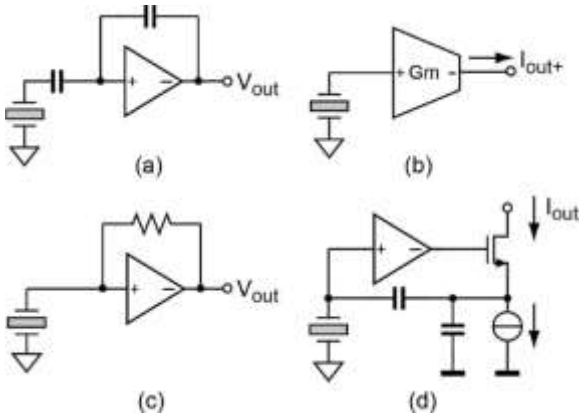

Figure 7: Ultrasound LNA topologies: (a) a capacitive-feedback voltage amplifier (VA); (b) a transconductance amplifier (TCA); (c) a resistive-feedback transimpedance amplifier (TIA); (d) a capacitive-feedback current amplifier (CA)

B. TIME-GAIN COMPENSATION AMPLIFIERS

There are two main categories of architectures for establishing a Time-Gain Compensation (TGC) amplifier in an integrated ultrasound system: programmable gain amplifiers (PGAs) with discrete gain steps and variable gain amplifiers (VGAs) with continuous gain control [6]; In both cases, the gain varies (approximately) exponentially with either the digital gain

code or the analog control voltage, resulting in a linear-in-dB time-gain profile.

PGAs offer a compelling advantage for integrated ultrasound systems as their precisely set gain steps ensure gain uniformity across a large array. These discrete gain steps can be defined using digitally-programmable ratiometric passive component networks, such as resistor attenuators, resistive feedback, capacitive feedback, and current-steering feedback. By distributing the PGA gain steps across multiple amplifier stages, coarse gain steps can be realized in the LNA, while fine gain steps are implemented in the succeeding PGA stages, extending the gain range while maintaining area efficiency. However, a downside of discrete-gain TGC is the switching transients between gain steps, which can introduce time-domain discontinuity and digital interference to the received signal, leading to image artifacts. This can be mitigated by reducing the gain steps to below 0.5 dB/step, but this increases silicon area due to the higher number of steps required to cover the desired gain range.

In contrast, VGAs implement TGC by continuously controlling the gain with an analog ramping voltage, avoiding switching transients associated with discrete gain steps. However, the translation from the linear control voltage to a decibel-scale gain profile increases circuit complexity, especially in the analog domain. One approach is to control the bias point of bipolar or MOS transistors operating in their non-linear region to achieve an approximately exponential transducer function. Yet, this method is limited in gain range and susceptible to process, voltage, and temperature variations, making it less practical for large ultrasound arrays. Another alternative is to use continuous interpolation between discrete gain steps. One such design, proposed by Gilbert (1991), employs a resistive ladder attenuator and an N-path current-controlled transconductance stage for smooth interpolation. However, its demand for multiple transconductance stages makes it less power and area efficient for modern compact ultrasound devices. A more efficient solution is to use a differential pair to smoothly steer the output current of an amplifier between different taps of a discrete-type feedback network. By controlling the voltage applied to the differential pair, continuous interpolation to the current gain of the amplifier can be achieved. This approach, first proposed in, has been recently demonstrated in a compact variable-gain ultrasound TIA with excellent gain linearity and noise-power efficiency .

C. ELEMENT-LEVEL DIGITIZATION

While most advanced integrated systems currently perform signal conditioning, pre-beamforming, or sub-aperture averaging in the analog domain before digitization, there is a growing trend to push the analog-to-digital interface closer to the transducer element. Element-level digitization offers several important advantages from a system perspective: it provides direct access to RF data from individual elements, removes the limitations imposed by fixed-aperture analog beamforming, enhances the flexibility of imaging algorithms, and allows for the integration of more powerful digital processing functions and artificial intelligence within a single ultrasound imaging device.

The main challenge in achieving element-level digitization is dealing with the mismatch between the large number of transducer elements and the limited power and area resources available for per-element ADCs. Researchers have undertaken various approaches to address this obstacle. For example, [8] demonstrated a digital beamformer using element-level Successive Approximation Register (SAR) ADCs, which proved advantageous in terms of power and area efficiency for direct-digitization solutions. Future efforts will focus on integrating analog or semi-digital Time-Gain Compensation (TGC) functions into the loop to extend the dynamic range of the ADC without compromising its efficiency.

Customized ADC techniques tailored for ultrasound signal processing are crucial for enabling element-level digitization. Lee et al. proposed a dynamic-bit-sharing technique that allows adjacent element-level SAR ADCs in a 2x2 subarray to share the most-significant-bits, resulting in power savings . Another hardware-sharing idea presented in involves a hybrid SAR/single-slope ADC that shares its ramp generator with adjacent channels in a 2x2 subarray, reducing the required area. Both approaches show promising area and power efficiency.

While the aforementioned approaches still place the analog front-end prior to the element-level ADC (Fig. 8a), a more innovative solution is to implement the analog-to-digital interface directly around the transducer element, effectively transforming it into an electromechanical filter within a closed-loop signal modulator. This concept was first demonstrated in, where a piezoelectric transducer element is used as a resonator in a second-order bandpass ΔΣ ADC (Fig. 8b). Alternatively, a CMUT element with capacitive impedance can act as a passive integrator in a continuous-time low-pass ΔΣ modulator (Fig. 8c), as described in . This approach eliminates the need for front-end analog processing and opens new possibilities for direct digitization at the element level.

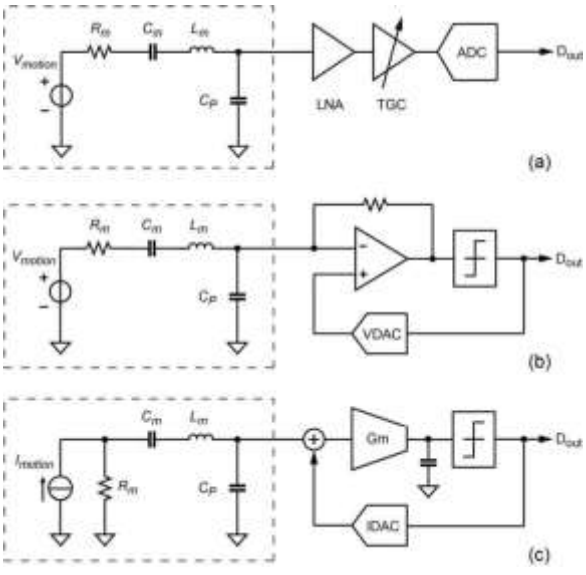

Figure 8: shows different element-level digitization topologies: (a) Stand-alone ADCs following an analog front-end ; (b) an element-level ADC using the transducer as a resonator in a bandpass ΔΣ modulator ; (c) an element-level ADC utilizing the transducer as a passive integrator in a lowpass ΔΣ modulator. The stand-alone ADC approach employs a conventional charge-redistribution capacitive DAC, which requires significant silicon area and hinders pitch-matching integration with the transducer array. To overcome this limitation, Chen et al. integrated a ΔΣ ADC with an analog front-end using a nanoscale CMOS process, fitting it within the area of a single CMUT element , though its energy efficiency is not yet competitive with the analog approach.

5. CONCLUSION

This paper provides a review of circuit solutions tailored for emerging ultrasound imaging devices, including 3D imaging catheters, portable ultrasound scanners, and wearable ultrasound patches. Despite the different operating principles of available transducer technologies (bulk piezoelectric transducers, CMUTs, and PMUTs), their electrical characteristics are quite similar, allowing for the application of similar circuit architectures. The focus has been on front-end building blocks that interface with the transducer elements, aiming to minimize power consumption and enhance performance, such as high-voltage pulsers for transmission and low-noise amplifiers and time-gain compensation for reception. Additionally, advanced techniques like multi-level pulsing and element-level digitization have been discussed.

Currently, most in-probe ASICs serve as interfaces between the transducer and conventional imaging systems, providing amplification for improved SNR and channel-count reduction for 3D imaging through multiplexing or sub-array beamforming. However, there is a growing trend towards full in-probe digitization , which allows for a robust digital

interface with the system and enables in-probe digital signal processing, leading to further data reduction. Standardized digital interfaces also facilitate integration with other physician support tools. This trend may ultimately lead to the integration of all front-end electronics on-chip within the probe, rendering imaging systems obsolete, and shifting image processing to software . This integration is crucial for reducing the size and cost of handheld ultrasound scanners compared to PCB-based solutions . Furthermore, it is essential for the future of wearable ultrasound devices , which could enable home use and long-term monitoring applications. These wearable devices will need to operate on small batteries and communicate wirelessly with devices like smartphones, demanding significant advances in power efficiency and data reduction, motivating further developments in integrated circuit design for ultrasound applications.

REFERENCES

[1] Bezek, C. D., & Goksel, O. (2023). Analytical estimation of beamforming speed-of-sound using transmission geometry. Ultrasonics, 107069.

[2] Chen, C., & Pertijs, M. A. (2021). Integrated transceivers for emerging medical ultrasound imaging devices: A review. IEEE Open Journal of the Solid-State Circuits Society, 1, 104-114.

[3] Ciecierski-Holmes, T., Singh, R., Axt, M., Brenner, S., & Barteit, S. (2022). Artificial intelligence for strengthening healthcare systems in low-and middle-income countries: a systematic scoping review. npj Digital Medicine, 5(1), 162.

[4] Gilbert, B. (1991, February). A low-noise wideband variable-gain amplifier using an interpolated ladder attenuator. In 1991 IEEE International Solid-State Circuits Conference. Digest of Technical Papers (pp. 280-281). IEEE.

[5] Golemati, S., & Cokkinos, D. D. (2022). Recent advances in vascular ultrasound imaging technology and their clinical implications. Ultrasonics, 119, 106599.

[6] Guo, P., Chang, Z. Y., Noothout, E., Vos, H. J., Bosch, J. G., de Jong, N., ... & Pertijs, M. A. (2022). A pitch-matched low-noise analog front-end with accurate continuous time-gain compensation for high-density ultrasound transducer arrays. IEEE Journal of Solid-State Circuits.

[6] Jeong, K., Yun, G., Choi, J., Choi, I., Son, J., Hwang, J. Y., ... & Je, M. (2023). A Wide-Bandwidth Ultrasound Receiver and On-Chip Ultrasound Transmitter for Ultrasound Capsule Endoscopy. IEEE Journal of Solid-State Circuits.

[7] Kim, J., Choi, W., Park, E. Y., Kang, Y., Lee, K. J., Kim, H. H., ... & Kim, C. (2019). Real-time photoacoustic thermometry combined with clinical ultrasound imaging and high-intensity focused ultrasound. IEEE Transactions on Biomedical Engineering, 66(12), 3330-3338.

[8] Kim, Y. J., Cho, S. E., Um, J. Y., Chae, M. K., Bang, J., Song, J., ... & Park, H. J. (2016). A single-chip 64-channel ultrasound RX-beamformer including analog front-end and an LUT for non-uniform ADC-sample-clock generation. IEEE Transactions on Biomedical Circuits and Systems, 11(1), 87-97.

[9] Kim, Y. H., Collins, J., Li, Z., Chinnadurai, P., Kapoor, A., Lin, C. H., & Mansi, T. (2022). Automated catheter tip repositioning for intra-cardiac echocardiography. International Journal of Computer Assisted Radiology and Surgery, 17(8), 1409-1417.

[10] Li, Y., Li, Y., Zhang, R., Li, S., Liu, Z., Zhang, J., & Fu, Y. (2023). Progress in wearable acoustical sensors for diagnostic applications. Biosensors and Bioelectronics, 115509.

[11] Marbach, J. A., Almufleh, A., Di Santo, P., Simard, T., Jung, R., Diemer, G., ... & Hibbert, B. (2020). A shifting paradigm: the role of focused cardiac ultrasound in bedside patient assessment. Chest, 158(5), 2107-2118.

[12] Novaresi, L., Malcovati, P., Mazzanti, A., & Bonizzoni, E. (2023). A Bipolar 3-Level High-Voltage Pulser for Highly

Integrated Ultrasound Imaging Systems. IEEE Transactions on Circuits and Systems II: Express Briefs.

[13] Pal, M., Maity, N. P., Baishya, S., & Maity, R. (2021). Performance analysis of nano-electro-mechanical-system ultrasonic sensor with fringing field effects. Transactions on Electrical and Electronic Materials, 22, 757-763.

[14] Pham, A. H., Berg, E. A. R., Veronesi, F., Fiorentini, S., Fatemi, A., Grenne, B., ... & Kiss, G. (2019, October). Fast ultrasound to ultrasound auto-registration for interventional cardiology. In 2019 IEEE International Ultrasonics Symposium (IUS) (pp. 16-19). IEEE.

[15] Rezvanitabar, A., Jung, G., Tekes, C., Carpenter, T. M., Cowell, D. M., Freear, S., & Degertekin, F. L. (2022). Integrated hybrid sub-aperture beamforming and time-division multiplexing for massive readout in ultrasound imaging. IEEE Transactions on Biomedical Circuits and Systems, 16(5), 972-980.

[16] Sadeghpour Shamsabadi, S. (2020). Piezoelectric Micromachined Ultrasound Transducer (pMUT) Array for Underwater Communication.

[17] Savoia, A. S., Mauti, B., & Caliano, G. (2020). Integration of two-dimensional MEMS ultrasonic transducer arrays with front-end electronics for medical ultrasound imaging. In Sensors and Microsystems: Proceedings of the 20th AISEM 2019 National Conference 20 (pp. 177-182). Springer International Publishing.

[18] Sehmbi, H., & Perlas, A. (2022). Basics of ultrasound imaging. In Regional Nerve Blocks in Anesthesia and Pain Therapy: Imaging-guided and Traditional Techniques (pp. 33-52). Cham: Springer International Publishing.

[19] Song, J., Zhang, Q., Zhou, L., Quan, Z., Wang, S., Liu, Z., ... & Yuchi, M. (2021). Design and implementation of a modular and scalable research platform for ultrasound computed tomography. IEEE transactions on ultrasonics, ferroelectrics, and frequency control, 69(1), 62-72.

[20] Wodnicki, R., Kang, H., Li, D., Stephens, D. N., Jung, H., Sun, Y., ... & Ferrara, K. W. (2022). Highly integrated multiplexing and buffering electronics for large aperture ultrasonic arrays. BME frontiers, 2022.

[21] Zhang, Y., & Demosthenous, A. (2021). Integrated circuits for medical ultrasound applications: Imaging and beyond. IEEE Transactions on Biomedical Circuits and Systems, 15(5), 838-858.

[22] Zhou, M., Chen, P., Mischi, M., Cantatore, E., & Harpe, P. (2021, September). The Impact of the Transmission Pulse Shape in Ultrasound Harmonic Imaging. In 2021 IEEE International Ultrasonics Symposium (IUS) (pp. 1-4). IEEE.